Ocean Dynamics (2001) 52: 51–57
DOI 10.1007/s102360100001

John A. T. Bye · Jörg-Olaf Wolff

Momentum transfer at the ocean–atmosphere interface: the wave basis for the inertial coupling approach

Received: 6 January 2001 / Accepted: 28 June 2001

Abstract The inertial coupling approach for the momentum transfer at the ocean–atmosphere interface, which is based on the assumption of a similarity hypothesis in which the ratio between the water and air reference velocities is equal to the square root of the ratio between the air and water densities, is reviewed using a wave model. In this model, the air and water reference velocities are identified, respectively, with the spectrally weighted phase velocity of the gravity waves and the Stokes velocity at the water roughness length, which are evaluated in terms of the dimensionless frequency limits in Toba's equilibrium spectrum. It is shown that the similarity hypothesis is approximately satisfied by the wave model over the range of wave ages encountered in typical sea states, and that the predicted values of the dimensionless surface drift velocity, the dimensionless water reference velocity, and the Charnock constant are in reasonable agreement with observational evidence. The application of the bulk relationship for the surface shear stress, derived from the inertial coupling hypothesis in general circulation modeling, is also discussed.

Keywords Air–sea momentum exchange · Wave model · Surface shear stress · Inertial coupling

1 Introduction

The formulation of the momentum transfer process across the air–sea interface is of central importance for the study of the coupled ocean–atmosphere. Most observational programs have been made in the atmospheric boundary layer, implicitly with the assumption that the small current velocities, in comparison with wind velocities, are of minor importance, serving only to make a small change in reference velocity to the system. This assertion was challenged by Bye (1995), who proposed that the neglect of the near-surface ocean dynamics, which are dominated by the gravity wave spectrum, may lead to a serious misrepresentation of the momentum transfer process. The basic reason was that the small surface current velocity used in the traditional formulation varies in space and time, and hence the surface shear stress which is obtained from a theoretical framework using this velocity is deficient, since the frame of reference for the coupled ocean–atmosphere system is the Earth reference frame (Bye and Wolff 1999). The formulation given in Bye (1995), which was called the inertial coupling relation, overcomes this deficiency and provides an expression for the surface shear stress relative to the Earth reference frame.

It is the purpose of this paper to review the basis of the inertial coupling relation using a wave model which involves a refinement of the analysis given in Bye (1988) and also an expression for the spectrally weighted phase velocity of the gravity wave spectrum. It will be emphasized that the inertial coupling hypothesis is grounded on observational studies on both sides of the air–sea interface, and follows naturally from traditional concepts of coupled frictional layers using the wave boundary layer model, presented below.

The main significance of the inertial coupling relation, however, is its interpretation in terms of the large-scale interaction of coupled fluids of large density contrast (Bye and Wolff 1999), which is also discussed later.

2 Formulation of the coupled frictional layers

The two basic profile relations which apply approximately near the sea surface are, in the air:

Responsible Editor: Dirk Olbers

J. A. T. Bye (✉)
School of Earth Sciences,
University of Melbourne, Victoria 3052, Australia
e-mail: jbye@unimelb.edu.au

J.-O. Wolff
ICBM, Universität Oldenburg,
Postfach 2503, 26111 Oldenburg, Germany
e-mail: wolff@icbm.de

$$u' = u_S + u_*/\kappa \ln z/z_0 \ , \quad (1)$$

and in the water:

$$u = u_R - w_*/\kappa \ln z/z_R, \quad z_R > z_0 \ , \quad (2)$$

in which the meteorological convention (z positive upwards) is used in the air, and oceanographical convention (z positive downwards) is used in the water, and $z = 0$ at the mean sea level. The friction velocities in air and water are, respectively, u_* and w_* where $u_* = (\tau_s/\rho')^{1/2}$ and $w_* = (\tau_s/\rho)^{1/2}$ in which ρ' and ρ are, respectively, the density of air and water, τ_s is the surface shear stress, u_S is the air velocity at $z = z_0$, u_R is the water velocity at $z = z_R$, and κ is von Karman's constant. Equation (1) would be expected to apply in the constant stress layer of a neutral atmosphere, and Eq. (2) has been observed in the constant stress layer of the ocean, even though wave motions were also present. As they stand, Eqs. (1) and (2) do not fully define the coupled system. This inadequacy can be overcome by defining a paired expression in the other fluid for each of the relations. For Eq. (1), the paired equation for water is:

$$u = u_S - w_*/\kappa \ln z/z_0 \ . \quad (3)$$

This technique, which was originally applied in Bye (1965), where simultaneous profiles in air and water were available, which had the property that $w_* = \varepsilon u_*$ where $\varepsilon = (\rho'/\rho)^{1/2}$, unambiguously defines the velocity, u_S, which is usually called the surface drift velocity, and also the air roughness length, z_0, which is usually just called the roughness length, although no physical reality is implied for the coordinate (u_S, z_0).

In practice, the drift speed of entities at the sea surface is influenced by many other factors, see, for example, Wu (1975). The pair of relations (Eqs. 1 and 3) is the description of the momentum coupling in the u_S reference frame.

For Eq. (2), the paired equation for air is:

$$u' = u'_R + u_*/\kappa \ln z/z_R \ , \quad (4)$$

where u'_R is the velocity in air at $z = z_R$, which can be expressed in terms of u_R by the relation:

$$u_R = \varepsilon\chi u'_R \ , \quad (5)$$

where χ is a constant. The substitution of Eq. (1) into Eq. (4), and Eq. (2) into Eq. (3) yields the relations between the velocities:

$$u_S = (1+\chi)/(1-\varepsilon\chi) w_*/\kappa \ln z_R/z_0 \quad (6)$$

and

$$u_R = \chi(1+\varepsilon)/(1+\chi) u_S \ . \quad (7)$$

In the inertial coupling relation, introduced in Bye (1995), Eq. (5) is written in the form:

$$u'_R = u_L + u_0 \quad (8)$$

and

$$u_R = \varepsilon u_L + u_0 \ , \quad (9)$$

in which u_0 is the nonwave-induced velocity common to both fluids, u_L is the wave-induced velocity in the air (the spectrally weighted phase velocity), and εu_L is the wave-induced velocity in the water (the spectrally integrated Stokes velocity). The choice of the coefficient, ε, in Eq. (9) ensures that Eqs. (2) and (4) are of similarity form. The substitution of Eqs. (8) and (9) in Eqs. (4) and (2), respectively, and the elimination of u_L yields:

$$u_* = C^{1/2}[u' - u_0 - (u - u_0)/\varepsilon] \ , \quad (10)$$

in which the drag coefficient, $C = 1/4(\kappa^2/\ln^2 z/z_R)$, and

$$u_0 = (u + \varepsilon u' - 2\varepsilon u_L)/(1+\varepsilon) \ , \quad (11)$$

and also from Eqs. (1) and (3) using Eq. (11), we have:

$$u_S = u_0 + 2\varepsilon u_L/(1+\varepsilon) \ , \quad (12)$$

which illustrates that the surface drift velocity also can be partitioned into a wave-induced and a nonwave-induced component. The implications of the inertial coupling hypothesis are discussed in Section 4.

3 The wave boundary layer model

The main purpose of this paper is to evaluate u_R and u'_R directly, using wave spectral estimates, and hence to check the validity of the partitioning of the velocities (Eqs. 8 and 9) on which the inertial coupling relation is based. We will assume that the wave spectrum is described by the Toba spectrum for wind-generated gravity waves (Toba 1973) and that nonwave-induced currents are absent ($u_0 = 0$). In this situation, Eqs. (8) and (9) predict that $\chi = 1$.

The estimate of u_R is obtained from an extension of the results presented in Bye (1988), which are based on the Toba spectrum, in which the vertical profile of the spectrally integrated Stokes velocity, u, in the oceanic surface layer is given by the relation:

$$u = \alpha' u_* \int_{K_0}^{K_1} K^{-1} e^{-2KZ} dK \ , \quad (13)$$

where $K = u_*^2\sigma^2/g^2$ and $Z = gz/u_*^2$ are the dimensionless wavenumber and depth, respectively, σ is the wave frequency, g is the acceleration of gravity, α' is identified as ε/κ, i.e., for $\kappa = 0.4$ and $\varepsilon = 0.034$, $\alpha = 0.085$, and the indices 1 and 0 indicate, respectively, the value of K corresponding to the upper and lower wave frequencies in the equilibrium range of the wave-frequency spectrum. On taking the integral of Eq. (13) we obtain:

$$u = \alpha' u_* \left[\ln K_1/K_0 + \sum_{n=1}^{\infty} (-2Z)^n (K_1^n - K_0^n)/(nn!) \right] \ , \quad (14)$$

where $u \to 0$ for $Z \to \infty$. Also, differentiation of Eq. (13) with respect to Z followed by integration over K yields:

$$\mathrm{d}u/\mathrm{d}Z = \alpha' u_*/Z(\mathrm{e}^{-2K_1 Z} - \mathrm{e}^{-2K_0 Z}) \ , \quad (15)$$

whence it follows that:

$$\mathrm{d}u/\mathrm{d}Z = -2\alpha' u_* K_1 \quad \text{for } Z \ll (2K_1)^{-1} \ll (2K_0)^{-1} \quad (16)$$

and

$$\mathrm{d}u/\mathrm{d}Z = -\alpha' u_*/Z \quad \text{for } (2K_1)^{-1} \ll Z \ll (2K_0)^{-1} \ , \quad (17)$$

such that immediately below the ocean surface the vertical distribution of Stokes velocity is described by a linear law, while deeper in the oceanic surface layer the logarithmic law applies. Now, if we assume that the momentum flux, w_*^2, in the oceanic surface layer remains constant as for a wall boundary layer, and identify the water roughness length as the depth of the transition from the linear to the logarithmic profile, where the nondimensional depth, $Z_R = (2K_1)^{-1}$, we find from Eq. (14) that the water reference velocity

$$u_R = w_*/\kappa \left[\ln K_1/K_0 + \sum_{n=1}^{\infty} (-1)^n (1 - (K_0/K_1)^n)/(nn!) \right]$$
$$\approx w_*/\kappa (\ln K_1/K_0 - 0.80), \quad K_1 \gg K_1 \ , \quad (18)$$

and

$$z_R = a_R u_*^2/g \quad (19)$$

is the water roughness length, where $a_R = Z_R$. Note that in Bye (1988) the constant term in Eq. (18), which is small in comparison with the log term for an extended wavenumber range, was omitted, i.e., the shear above $z = z_R$, which is small in comparison with the logarithmic shear, was neglected (and also a nonstandard notation was used in which the air roughness length was denoted by z_0' instead of z_0 and the water roughness length was denoted by z_0 instead of z_R).

The spectrally weighted phase velocity of the gravity waves, $u_R' = g/\bar{\sigma}$, where $\bar{\sigma}$ is the mean wave frequency specified by the equality

$$\bar{\sigma}^2 \int_0^{\infty} S(\sigma)\mathrm{d}\sigma = \int_0^{\infty} \sigma^2 S(\sigma)\mathrm{d}\sigma \ , \quad (20)$$

in which $S(\sigma)$ is the wave frequency spectrum specified according to Toba (1973), as

$$\begin{aligned} S(\sigma) &= 0, \quad \sigma > \sigma_1 \text{ and } \sigma < \sigma_0 \\ S(\sigma) &= \alpha u_*^2 g \sigma^{-4}, \quad \sigma_1 \geq \sigma \geq \sigma_0 \ , \end{aligned} \quad (21)$$

where σ_0 and σ_1 are, respectively, the lowest and highest frequencies of the equilibrium range in the spectrum, and $\alpha \approx 0.096$ is Toba's constant. Substitution of Eqs. (21) into Eq. (20) to obtain $\bar{\sigma}$, and hence u_R' yields:

$$u_R' = u_*/(3K_0)^{1/2} \left[(1 - (K_0/K_1)^{3/2})/(1 - (K_0/K_1)^{1/2} \right]^{1/2}$$
$$\approx u_*/(3K_0)^{1/2}, \quad K_1 \gg K_0 \ , \quad (22)$$

or, from the approximate expression, equivalently, $u_R = c_0/\sqrt{3}$, in which $c_0 = g/\sigma_0$ is the wavespeed of the lowest frequency (σ_0) wave. The spectral expressions for u_R and u_R' can be used to find χ from Eq. (5), which yields:

$$\chi = (3K_0)^{1/2} (\ln K_1/K_0 - 0.80)/\kappa, \quad K_1 \gg K_0 \ . \quad (23)$$

Equation (23) is an expression for χ in terms of the wave age, $c_0/u_* = K_0^{-1/2}$, and also the Charnock parameter for the water roughness length, $a_R = (2K_1)^{-1}$. Figure 1 shows χ evaluated from Eq. (23) over a range of wave ages, and $K_1 = 0.5$ ($a_R = 1$), which is the upper limit of K_1 given in Phillips (1985), and is also equal to that found by Bourrassa (2000) in a reevaluation of observed water velocity profiles. It is apparent that over the approximate wave age range ($30 > c_0/u_* > 5$), $\chi \approx 1$. The evaluation of χ using the exact expressions for u_R and u_R' has a somewhat smaller variation of χ (1.4–0.7) over the same range of wave ages, and, as it should, indicates that $\chi \to 0$ for $K_0 \to K_1$. Thus, the Toba spectrum wave dynamics are consistent with a wave-dominant environment, which approximately satisfies the similarity hypothesis on which the inertial coupling relation is based, and in which nonlocal processes are unimportant. This conclusion, although necessarily imprecise owing to the simple model of the wave spectrum used, strongly supports the partitioning of the velocities (u_R and u_R') used in Eqs. (8) and (9). The sensitivity to K_1 is illustrated in Fig. 1 by the evaluation of χ for $K_1 = 0.35$ ($a_R = 1.4$) which is the mid-range of K_1 given in Phillips (1985), and which was also used in Bye (1988).

3.1 Comparison of the similarity model with observational data

A check on the validity of the similarity model ($\chi = 1$) can be obtained from field measurements of the vertical profiles of the mean velocity in the surface layers of air and water (see Bye 1965, 1987; Churchill and Csanady 1983). On substituting Eq. (5) in Eq. (16), we obtain the nondimensional water reference velocity ratio:

$$u_R/w_* = (3K_0)^{-1/2} \ , \quad (24)$$

from which Eq. (7) yields the nondimensional surface drift ratio:

$$u_S/w_* = 2/(1+\varepsilon)(3K_0)^{-1/2} \ . \quad (25)$$

For $K_1 = 0.5$, Eqs. (24) and (25) yield $u_R/w_* = 11$, and $u_S/w_* = 21$. For comparison, the experimental estimates are in the ranges 7–23 (mean 11), and 19–35 (mean 25), respectively (Bye 1988).

The set of relations for the wave model (Eqs. 6, 19, and 25) also enable the Charnock parameter for air (Charnock's constant) to be predicted; the result is:

$$a_0 = 1/(2K_1) \exp\left[-\kappa(1-\varepsilon)/(1+\varepsilon)(3K_0)^{-1/2} \right] \ , \quad (26)$$

where $a_0 = Z_0$, and $z_0 = a_0 u_*^2/g$. On evaluating Eq. (26) for $K_1 = 0.5$, we obtain $a_0 = 0.017$, which is a magnitude similar to observational estimates (Garratt 1992).

3.2 Extension to more general conditions

The wave model can be extended to include the transfer of momentum by turbulent (Ekman) shear in addition to wave (Stokes) shear, by specifying the momentum flux to the waves as a fraction γ^2 of the total wind stress. In this case, all the results presented above remain valid with the reservation that u_* should now be replaced by γu_*. Then, on adding an Ekman velocity, u_E, to the Stokes velocity of Eq. (25), we obtain:

$$u_R = \gamma u_R + u_E \quad , \tag{27}$$

which is identical with Eq. (9), since by definition, the wave-induced velocity is the Stokes velocity, $\varepsilon u_L = \gamma u_R$, and the nonwave-induced velocity is the Ekman velocity, $u_0 = u_E$. On defining the ratio of the Stokes velocity to the Ekman velocity, $R = \varepsilon u_L/u_0$, Eq. (27) yields:

$$\gamma = (1 + R^{-1})^{-1} \quad , \tag{28}$$

whence, as it must, $\gamma = 0$ at $R = 0$ (the case of no Stokes velocity) and $\gamma = 1$ at $R = \pm\infty$ (the case of no Ekman velocity). If, for example, the Stokes drift velocity and the Ekman drift velocity are of the same magnitude ($R = 1$), it follows from Eq. (28) that $\gamma^2 = 0.25$, which is in good agreement with the estimates of γ^2 presented in Phillips (1977). Note also that for the partition of momentum flux described above, the wave ages of the basic analysis, e.g., in Fig. 1, would be reduced by the factor (γ).

3.3 Wave breaking effects in the wave boundary layer

The extension of the wave boundary layer model to include both Stokes and Ekman surface drift accommodates in a basic way all the key processes operating in the upper ocean dynamics, in particular the role of wave-breaking, which was examined by Craig and Banner (1994), Craig (1996) and Melsom (1996), who, on theoretical grounds, demonstrated that wave-breaking significantly enhances the mean velocity. In addition, Craig and Banner (1994) and Craig (1996) established that the mean velocity in the near-surface layer is approximately linear with depth, while the turbulent kinetic energy and the turbulent kinetic energy dissipation decay with depth at powers several times greater than 1. In other words, the vertical structure of the near-surface layer, which is created by wave-breaking, is quite different from that inherent in the logarithmic layer, as confirmed by experimental data (Kitaigorodskii et al. 1983; Thorpe 1984; Agrawal et al. 1992; Anis and Moum 1992; Drennan et al. 1992; Osborn et al. 1992; Terray et al. 1996). This linear velocity profile is also predicted by the wave boundary layer model (see Sect. 3), although wave-breaking processes are not explicitly considered. That is, models, each of which describes the mean drift from a different viewpoint, provide identical (in a qualitative respect) results. This should be kept in mind when interpreting experimental data, in particular the data of Csanady (1984), who suggested that the linear velocity profile detected in the surface layer was due to breaking waves.

4 The inertial coupling relation

The extension of the wave model (see Sect. 3.2) has justified the general form of the partitioning of the reference velocities (u_R and u'_R) used in the one-dimensional inertial coupling relation (Eq. 10). The two-dimensional inertial coupling relation of Bye (1995) follows directly on relaxing the assumption that the Stokes velocities and the Ekman velocities are collinear, which yields:

$$\tau_S = \rho_1 C \,|\, u' - u_0 - (u - u_0)/\varepsilon \,|\, [u' - u_0 - (u - u_0)/\varepsilon] \tag{29}$$

and

$$u_0 = (u + \varepsilon u' - 2\varepsilon u_L)/(1 + \varepsilon) \quad , \tag{30}$$

in which

$$u'_R = u_L + u_0 \tag{31}$$

and

$$u_R = \varepsilon u_L + u_0 \quad . \tag{32}$$

On substituting Eq. (30) into Eq. (29) we also obtain:

$$\tau_S = \rho_1 [2/(1 + \varepsilon)]^2 C \,|\, u' - u - (1 - \varepsilon) u_L \,| \times [u' - u - (1 - \varepsilon) u_L] \quad . \tag{33}$$

Equation (29) demonstrates the key property of the inertial coupling relation that the surface shear stress is expressed using velocities relative to the Ekman velocity (u_0) common to both fluids, and Eq. (33) is the corresponding relation in terms of the wave-induced velocity.

Equation (33) is a general relation for the surface shear stress, which shows that the presence of the wavefield can give rise to an upward transfer of momentum across the sea surface. Note that the form of Eq. (33) accommodates waves and wind of different orientations, since it is based on the partition of the reference velocities (Eqs. 31 and 32) used in the bulk formula. In this important respect it differs from the traditional approach to the partition of the total surface shear stress (essentially through the drag coefficient, rather than the velocities, used in the bulk formula) into a turbulent shear stress, wave-induced shear stress, and a viscous stress, e.g., Phillips (1977) and Makin and Kudryavtsev (1999).

Upward momentum transfer from the ocean to the atmosphere has recently been observed in field measurements (Smedman et al. 1994; Drennan et al. 1999) in situations where swell is propagating into regions of light wind. Equation (33) indicates that this is a generic

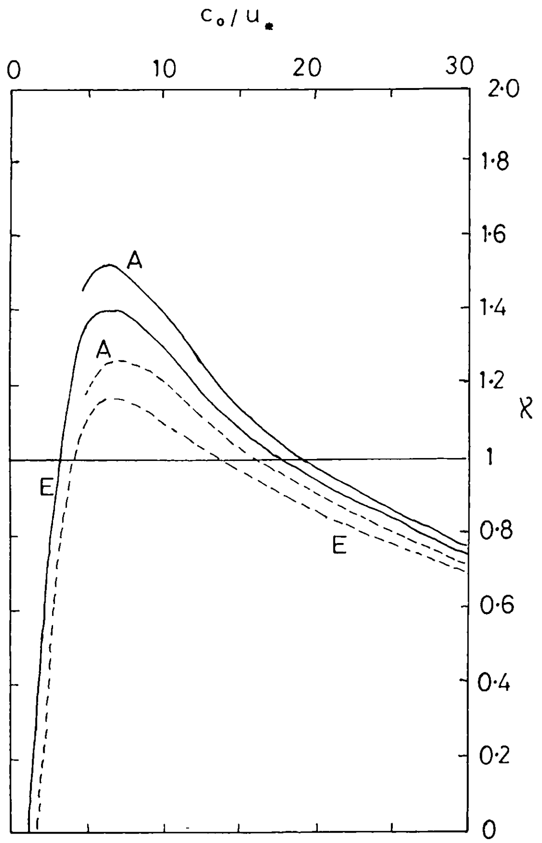

Fig. 1 The parameter χ as a function of wave age, c_0/u_*, for: $K_1 = 0.5$ ($a_R = 1$) solid curve, and $K_1 = 0.35$ ($a_R = 1.4$) dashed curve. E denotes evaluation from the exact solution, and A denotes evaluation from Eq. (23)

Values of χ (Table of values used in Fig. 1)

c_0/u_*	Exact	Eq. (23)	
1.4	0	–	$K_1 = 0.5$
2.5	0.79	–	
5	1.34	1.47	
5.8	–	1.51	(Maximum)
7	1.39	1.50	
10	1.30	1.38	
15	1.09	1.14	
17	1.02	1.06	
20	0.94	0.97	
30	0.74	0.76	
1.7	0	–	$K_1 = 0.35$
2.5	0.48	–	
5	1.09	1.17	
6.8	–	1.27	(Maximum)
7	1.17	1.27	
10	1.14	1.22	
15	0.98	1.03	
17	0.92	0.97	
20	0.86	0.90	
30	0.70	0.71	

process, and that the wavefield is of first-order importance to the dynamics of the ocean general circulation. In particular, it suggests that the Ekman dynamics are not essentially controlled by the wind, but by the wind and the wavefield, each being of similar importance. This places much more importance on wave modeling in general circulation studies than has been suggested by other studies, e.g., McWilliams and Restrepo (1999).

Equation (30) links the two representations of τ_S. The relations apply within the wave boundary layer, which extends upwards and downwards from the interface. At the edges of the wave boundary layer ($z = z_B$), the fluid velocity tends to the free stream velocity, thus $u_1 = u'(z_B)$ is the surface wind, and $u_2 = u(z_B)$ is the surface current. In the following discussion, the relations will be applied at $z = z_B$. The incorporation of the wave-boundary layer in the planetary boundary layer is discussed in a separate paper (Bye 2001), in which the steady-state Ekman solution for the two fluids coupled by Eq. (29) is presented.

We consider next the inertial coupling relation in the frame of reference of the surface shear stress, and assume that τ_s lies along the Ox axis. Then, from Eqs. (29) and (30), we obtain:

$$v = \varepsilon v_L + v_0 \tag{34}$$

and

$$v' = v_L + v_0 \ , \tag{35}$$

such that the normal velocities in air and water, respectively, v' and v are constant, and all the velocity shears lie along Ox. Next, on introducing the relation between the Stokes shear and the Eulerian shear:

$$\varepsilon u_L = r(u_0 - u_2) \ ,$$

where r is a constant (note that for $u_2 = 0$, $r = R$, see Sect. 3.2), Eq. (29) and Eq. (30) reduce to scalar expressions in which τ_{sx} and u_L are functions of the surface wind relative to the surface current, namely,

$$\tau_{sx} = \rho_1 C|F|(F)|u_1 - u_2|(u_1 - u_2) \ , \tag{36}$$

where $F = 2(r+1)/(1+\varepsilon+2r)$, and

$$u_L = r/(1+\varepsilon+2r)(u_1 - u_2) \ . \tag{37}$$

In a frame of reference in each fluid moving at the respective normal velocities, these relations are a formally complete description of the momentum exchange process. The normal circulation acts solely to *ventilate the stress field*, and from Eqs. (34) and (35), it consists of both the Eulerian and Stokes components of the dynamics, the total normal velocities being determined by the Ekman dynamics, as discussed in Bye (2001). Furthermore, in horizontally homogeneous conditions in which the surface shear stress is a constant vector, they would be also valid at a fixed measurement station. Thus, the classical drag law description of the near-surface momentum transfer is the limiting form of the more general inertial coupling relation, applicable in horizontally homogeneous conditions. Two limiting conditions are the following:

1. The surface current (u_2) is equal to the Ekman velocity (u_0), common to both fluids ($r = \pm\infty$). Here, it

is assumed that the shear in the wave boundary layer is due only to the wavefield, and the role of the surface current is solely that of a moving reference. In this local reference frame, Eq. (36) and Eq. (37) predict that

$$\tau_{sx} = \rho_1 C|u_1 - u_2|(u_1 - u_2) \tag{38}$$

and

$$u_L = \frac{1}{2}(u_1 - u_2) \ . \tag{39}$$

2. The wavefield is of negligible importance ($r = 0$). Here, Eq. (36) reduces to the relation:

$$\tau_{sx} = \rho_1 [2/(1+\varepsilon)]^2 C|u_1 - u_2|(u_1 - u_2) \ , \tag{40}$$

which is of form similar to Eq. (38), but in which τ_{sx} would be enhanced for the same drag coefficient (C), due to the Ekman shear in the water.

The *familiar forms* (Eqs. 36 and 37), however, obscure the fundamental structure of the inertial coupling relation, as discussed at the beginning of this section, and applied to general circulation modeling in the next section.

5 The application of the inertial coupling relation in general circulation modeling

In order to apply the inertial coupling relation in general circulation models, u_L in Eq. (33) must be predicted using a wave model. This is achieved by setting $u_0 = 0$ in Eq. (30), i.e., the analysis which generates the wavefield, by definition, is expressed in the Earth's reference frame. The resulting equation is of the form (Bye and Wolff 1999):

$$\varepsilon u_L = \frac{1}{2}(\varepsilon[u_1] + \{u_2\}) \ , \tag{41}$$

where $[u_1]$ and $\{u_2\}$ denote, respectively, appropriate two-dimensional spatial-temporal averages of the surface wind and surface current. Equation (41) can be directly substituted into Eq. (33) to obtain the surface shear stress, which was denoted by τ_{s0} in Bye and Wolff (1999). The *instantaneous* nonwave-induced velocity (u_0) may also be evaluated from Eq. (30) using the instantaneous velocities (u_1) and (u_2), which yields:

$$u_0 = ((u_2 - \{u_2\}) + \varepsilon(u_1 - [u_1]))/(1+\varepsilon) \ , \tag{42}$$

and on substituting for u_0 in Eq. (29), we find that the averages of the surface wind and the surface current satisfy the relation

$$\tau_{s0} = \rho_1 C|[u_1] - \{u_2\}/\varepsilon|([u_1] - \{u_2\}/\varepsilon) \ . \tag{43}$$

Equation (41) is, in effect, a wave model. A simple recipe in which a short moving average of the surface wind, and a long moving average of the surface current are used offers an approximate working expression for u_L (Bye and Wolff 1999). This procedure recognizes that u_L incorporates both a contribution from wind-waves and swell. It is clearly of importance to develop more sophisticated relations for u_L, using spectral wave models that can be run as an integral part of coupled general circulation models.

6 Conclusion

The above analysis unifies the processes occurring across the air–sea interface, which separates two fluids of large density contrast. It is clear that it is necessary to consider the problem in a multiple reference framework, which can accommodate all aspects of the momentum exchange, whereas on using the local reference frame, only that part of the exchange process which can be represented by the three-dimensional turbulent fluctuations is considered. The implications of extending the representation to include the two-dimensional turbulence of the two fluids are far-reaching (Bye and Wolff 1999). This paper endeavors to provide a physical interpretation of the inertial coupling process on which these arguments are based in terms of the wave dynamics of the near-surface layer.

Acknowledgements This work was begun at the Flinders University of South Australia during the stay of Professor Boris Kagan, who initiated the analysis to check the similarity hypothesis used in the inertial coupling relation presented in Sect. 3. Partial support for this study was obtained through a travel grant for Professor Kagan from the Department of Industry, Science, and Tourism, Australia, under the Bilateral Science and Technology Collaboration Program. Helpful comments by two anonymous reviewers are also acknowledged.

References

Agrawal YC, Terray EA, Donelan MA, Hwang PA, Williams AJ, Drennan W, Kahma K, Kitaigorodskii S (1992) Enhanced dissipation of kinetic energy beneath breaking waves. Nature 359: 219–220

Anis A, Moum JN (1992) The superadiabatic surface layer of the ocean during convection. J Phys Oceanogr 22: 1221–1227

Bourrassa MA (2000) Shear stress model for the aqueous boundary layer near the air–sea interface. J Geophys Res 105: 1167–1176

Bye JAT (1965) Wind-driven circulation in unstratified lakes. Limnol Oceanogr 10: 451–458

Bye JAT (1987) Observations of drift velocity, wind and temperature profiles on the San Diego Model Yacht Pond (1965–1967). Cruise Rep. 12 Flinders Institute for Atmospheric and Marine Sciences. The Flinders University of South Australia

Bye JAT (1988) The coupling of wave drift and wind velocity profiles. J Mar Res 46: 457–472

Bye JAT (1995) Inertial coupling of fluids of large density contrast. Phys Lett (A) 202: 222–224

Bye JAT (2001) Inertially coupled Ekman layers. Dynamics of Oceans and Atmospheres (in press)

Bye JAT, Wolff J-O (1999) Atmosphere–ocean momentum exchange in general circulation models. J Phys Oceanogr 29: 671–692

Churchill JH, Csanady GT (1983) Near-surface measurements of quasi-Lagrangian velocities in open water. J Phys Oceanogr 13: 1669–1680

Craig PD (1996) Velocity profiles and surface roughness under breaking waves. J Geophys Res 101: 1265–1277

Craig PD, Banner ML (1994) Modelling wave-enhanced turbulence in the ocean surface layer. J Phys Oceanogr 24: 2546–2259

Csanady GT (1984) The free surface turbulent shear layer. J Phys Oceanogr 14: 402–411
Drennan WM, Kahma KK, Terray EA, Donelan MA, Kitaigorodskii SA (1992) Observations of the enhancement of kinetic energy dissipation beneath breaking wind waves. In: Banner ML, Grimshaw RHJ (eds) Breaking Waves. Springer Berlin Heidelberg New York, pp 95–101
Drennan WM, Kahma KK, Donelan MA (1999) On momentum flux and velocity spectra over waves. Boundary-Layer Met 92: 489–515
Garratt JR (1992) The atmospheric boundary layer. Cambridge University Press, Cambridge, 316 pp
Kitaigorodskii SA, Donelan MA, Lumley JL, Terray EA (1983) Wave turbulence interactions in the upper ocean, II: Statistical characteristics of wave and turbulent components of the random velocity field in the marine surface layer. J Phys Oceanogr 13: 1988–1999
Makin VK, Kudryavtsev VN (1999) Coupled sea surface-atmosphere model 1. Wind over waves coupling. J Geophys Res 104: 7613–7623
McWilliams JC, Restropo JM (1999) The wave-driven ocean circulation. J Phys Oceanogr 29: 2523–2540
Melsom A (1996) Effects of wave breaking on the surface drift. J Geophys Res 101: 12071–12078
Osborn T, Farmer DM, Vagle S, Thorpe SA, Cure M (1992) Measurements of bubble plumes and turbulence from a submarine. Atmos Ocean 30: 419–440
Phillips OM (1977) The dynamics of the upper ocean, 2nd edn., Cambridge University Press, New York, 336 pp
Phillips OM (1985) Spectral and statistical properties of the equilibrium range in wind-generated gravity waves. J Fluid Mech 156: 505–531
Smedman AS, Tjernstrom M, Hogstrom U (1994) The near-neutral marine atmospheric boundary layer with no surface shearing stress: a case study. J Atmos Sci 51: 3399–3411
Terray EA, Donelan MA, Agrawal YC, Drennan WM, Kahma KK, Williams AJ, Hwang PA, Kitaigorodskii SA (1996) Estimates of kinetic energy dissipation under breaking waves. J Phys Oceanogr 26: 792–807
Thorpe SA (1984) On the determination of K_v in the near-surface ocean from acoustic measurements of bubbles. J Phys Oceanogr 14: 855–863
Toba Y (1973) Local balance in the air–sea processes, III. On the spectrum of wind waves. J Oceanogr Soc Jpn 29: 209–220
Wu J (1975) Wind-induced drift currents. J Fluid Mech 65: 49–70